International Society for Biofabrication
PURPOSE-LED PUBLISHING™

PAPER

A 3D printed PCL/hydrogel construct with zone-specific biochemical composition mimicking that of the meniscus

To cite this article: Gokhan Bahcecioglu *et al* 2019 *Biofabrication* **11** 025002

View the article online for updates and enhancements.

You may also like

- Current advances in engineering meniscal tissues: insights into 3D printing, injectable hydrogels and physical stimulation based strategies
Ashutosh Bandyopadhyay, Baishali Ghibhela and Biman B Mandal
- Regional-specific meniscal extracellular matrix hydrogels and their effects on cell–matrix interactions of fibrochondrocytes
Jinglei Wu, Jiazhu Xu, Yihui Huang et al.
- Nanofiber configuration affects biological performance of decellularized meniscus extracellular matrix incorporated electrospun scaffolds
Haiyan Li, Xiaoyu Wang, Jiajie Liu et al.

GAS

BreathSpec®

The combination of GC and IMS enables a physical separation to detect volatiles without pre-concentration directly sampled from human breath.

Our GC-IMS based analyzer allows instant breath sampling and analysis of volatiles in minutes.

The transportable GC-IMS facilitates versatile sampling incl. direct exhalation, syringe based and also gas bags for sampling of breath and static body headspace (oral/nasal/skin).

▶▶▶ click for more details

This content was downloaded from IP address 46.221.3.98 on 27/02/2026 at 10:57

Biofabrication

PAPER

A 3D printed PCL/hydrogel construct with zone-specific biochemical composition mimicking that of the meniscus

RECEIVED
10 August 2018

REVISED
20 November 2018

ACCEPTED FOR PUBLICATION
7 December 2018

PUBLISHED
16 January 2019

Gokhan Bahcecioglu[1,2,3], **Nesrin Hasirci**[1,3,4], **Bahar Bilgen**[5,6,†] and **Vasif Hasirci**[1,2,3,7,8,†]

[1] BIOMATEN, METU Center of Excellence in Biomaterials and Tissue Engineering, Middle East Technical University, Ankara, Turkey
[2] Department of Biological Sciences, Middle East Technical University, Ankara, Turkey
[3] Department of Biotechnology, Middle East Technical University, Ankara, Turkey
[4] Department of Chemistry, Middle East Technical University, Ankara, Turkey
[5] Providence VA Medical Center, Providence, RI, United States of America
[6] Department of Orthopaedics, The Warren Alpert Medical School of Brown University and Rhode Island Hospital, Providence, RI, United States of America
[7] Department of Medical Engineering, Acıbadem Mehmet Ali Aydınlar University, Istanbul, Turkey
[8] Author to whom any correspondence should be addressed.
[†] Last authors.

E-mail: vhasirci@metu.edu.tr

Keywords: 3D printing, PCL, GelMA, agarose, zonal biochemical composition, dynamic stimulation

Supplementary material for this article is available online

Abstract

Engineering the meniscus is challenging due to its bizonal structure; the tissue is cartilaginous at the inner portion and fibrous at the outer portion. Here, we constructed an artificial meniscus mimicking the biochemical organization of the native tissue by 3D printing a meniscus shaped PCL scaffold and then impregnating it with agarose (Ag) and gelatin methacrylate (GelMA) hydrogels in the inner and outer regions, respectively. After incubating the constructs loaded with porcine fibrochondrocytes for 8 weeks, we demonstrated that presence of Ag enhanced glycosaminoglycan (GAG) production by about 4 fold ($p < 0.001$), while GelMA enhanced collagen production by about 50 fold ($p < 0.001$). In order to mimic the physiological loading environment, meniscus shaped PCL/hydrogel constructs were dynamically stimulated at strain levels gradually increasing from the outer region (2% of initial thickness) towards the inner region (10%). Incorporation of hydrogels protected the cells from the mechanical damage caused by dynamic stress. Dynamic stimulation resulted in increased ratio of collagen type II (COL 2) in the Ag-impregnated inner region (from 50% to 60% of total collagen), and increased ratio of collagen type I (COL 1) in the GelMA-impregnated outer region (from 60% to 70%). We were able to engineer a meniscus, which is cartilage-like at the inner portion and fibrocartilage-like at the outer portion. Our construct has a potential for use as a substitute for total meniscus replacement.

1. Introduction

Meniscus is a wedge shaped, semilunar fibrocartilaginous tissue that plays roles in load bearing and transmission, and joint lubrication and stability. The tissue is vascular and fibrous (type I collagen (COL 1) constitutes 70%–80% of the collagen) in the outer region, and avascular and cartilaginous (type II collagen (COL 2) constitutes 50%–60% of the collagen) in the inner region [1, 2]. Glycosaminoglycans (GAGs) are also more abundant in the inner region of the meniscus (2%–4% of dry weight) than the outer region (1%) [2, 3]. During daily activities the knee joint is subject to a load 2.7–4.9 times the body weight [4], and 45%–75% of this load is transmitted to the meniscus [5]. The meniscus is subject to axial compressive and radial tensile stresses at 12% and 1% strain levels, respectively, and the magnitude of strain increases from the outer region towards the inner region [6].

A functional, engineered meniscus should mimic the biochemical organization of the native tissue and have sufficient mechanical properties to withstand the stress exerted on the knee joint [7]. There have been

© 2019 IOP Publishing Ltd

many attempts to engineer constructs for total replacement of the meniscus. Lyophilized foam-based constructs have poor mechanical properties and are suitable for use in partial replacement of the meniscus [8–10]. Electrospun mats are too thin to be considered for total meniscal replacement although some have good mechanical properties and others can mimic the biochemical composition of the meniscus [11, 12].

3D printed constructs can be produced in the desired shape and architecture, and with appropriate mechanical properties. Poly(ε-caprolactone) (PCL) is the material of choice in melt-based extrusion printing systems because of its biocompatibility, relatively low melting temperature (60 °C), and good rheological and viscoelastic properties [13–15]. One major drawback of PCL is that it lacks biofunctional groups necessary for cells to adhere. Hence, most of the PCL-based meniscal constructs fail to mimic the biochemical composition of the native meniscus [16–19]. Lee and colleagues have succeeded to engineer a construct with a cartilaginous inner portion and a fibrous outer portion by tethering microspheres loaded with transforming growth factor (TGF)-β3 and connective tissue growth factor (CTGF) on the respective regions of the PCL scaffolds [20]. However, these and other 3D printed PCL-based constructs result in degeneration of the underlying cartilage after being implanted, mainly because of friction between the material and the tissue [19, 20].

A meniscal construct with zonal variation can also be produced using hydrogels capable of inducing chondrogenic and fibrogenic activity in the inner and outer regions of the 3D printed PCL, respectively. Recently, our group and others have shown that agarose (Ag) is chondrogenic, while gelatin methacrylate (GelMA) is fibrogenic [2, 16]. In addition, reports show that gelatin induces angiogenesis [21, 22], while Ag does not support it because of the limited cell spreading on this gel [23]. The soft, hydrated hydrogels would also serve as a cushion and protect the articular cartilage from damage resulting from the mechanical load exerted on the knee [24].

The aim of this study was to engineer a meniscal construct that would have appropriate mechanical properties and a biochemical composition closely resembling that of meniscus. We printed a meniscus shaped PCL scaffold, and impregnated its inner region with Ag to induce chondrogenic phenotype and its outer region with GelMA to induce fibrogenic phenotype. In order to test the response of the constructs to physiologically relevant mechanical loads, a special loading platen that would create a biaxial stress at 2% compressive axial strain and 1% radial tensile strain in the outer region of the constructs and 10% compressive axial strain and 5% radial tensile strain in the inner region was used. Thus, the testing system would mimic physiological loading and provide valuable information about the potential performance of the constructs in animal and clinical settings. This study is unique in that it is the first to show that two different hydrogels can be used on 3D printed PCL scaffolds to create a biochemical composition closely resembling that of the meniscus.

2. Materials and methods

2.1. Tissue and cell harvest

Menisci were harvested from postmortem Yorkshire pigs (female, 2 months old) according to Lifespan Institutional Animal Care and Use Committee (IACUC) Policy for the Responsible Conduct of Animal Research and Use of Central Research Facilities (USA) with no review requirement.

In order to isolate fibrochondrocytes, menisci were minced, and incubated in type II collagenase (0.15%, w/v) at 37 °C overnight and then in growth media (DMEM-F12 (1:1) containing 10% FBS, 100 U ml^{-1} penicillin/streptomycin, 1% ITS + Premix, and 1 μg ml^{-1} amphotericin B (all Thermo Fisher Scientific, USA)) to allow migration of cells to tissue culture flasks [2]. Cells were expanded, treated with trypsin at confluence, frozen and stored at −80 °C until use. Porcine fibrochondrocytes were used to evaluate the scaffolds *in vitro*, as the preliminary step for the *in vivo* studies in a pig model that are being planned as a follow up of this study.

2.2. Preparation of the constructs

2.2.1. Preparation of PCL scaffolds

Poly(ε-caprolactone) (PCL) (Mw: 70–90 kDa, Sigma, USA) was 3D printed using Bioscaffolder system (SYS + ENG, Germany), and PrimCAM software (Switzerland) was used to create the interior design of the scaffolds (strand distance: 1 mm, strand orientation: 0/90°). Models were designed using the SketchUp software (Google inc., USA) in the shapes of a square prism (4 mm × 4 mm × 3 mm) for compressive testing, a rectangular prism (20 mm × 5 mm × 3 mm) for tensile testing, and meniscus (outer diameter: 30 mm, height at periphery: 5 mm, inner diameter: 10 mm). The models were converted to stereolithography (STL) file formats and printed.

2.2.2. Preparation of GelMA

GelMA was produced as described previously [2, 25]. Briefly, gelatin (from bovine skin, 225 Bloom, Sigma-Aldrich, USA) solution (10% w/v, in PBS, pH 7.2) and methacrylic anhydride (MA) (Sigma-Aldrich) were mixed in a proportion of 7:1 (Gelatin:MA, v/v) and incubated at 50 °C for 1.5 h, dialyzed against phosphate buffer (pH 7.2) for 3 days to remove unreacted MA, and freeze-dried at −80 °C. The resulting powder was sterilized with ethylene oxide and stored at −20 °C until use.

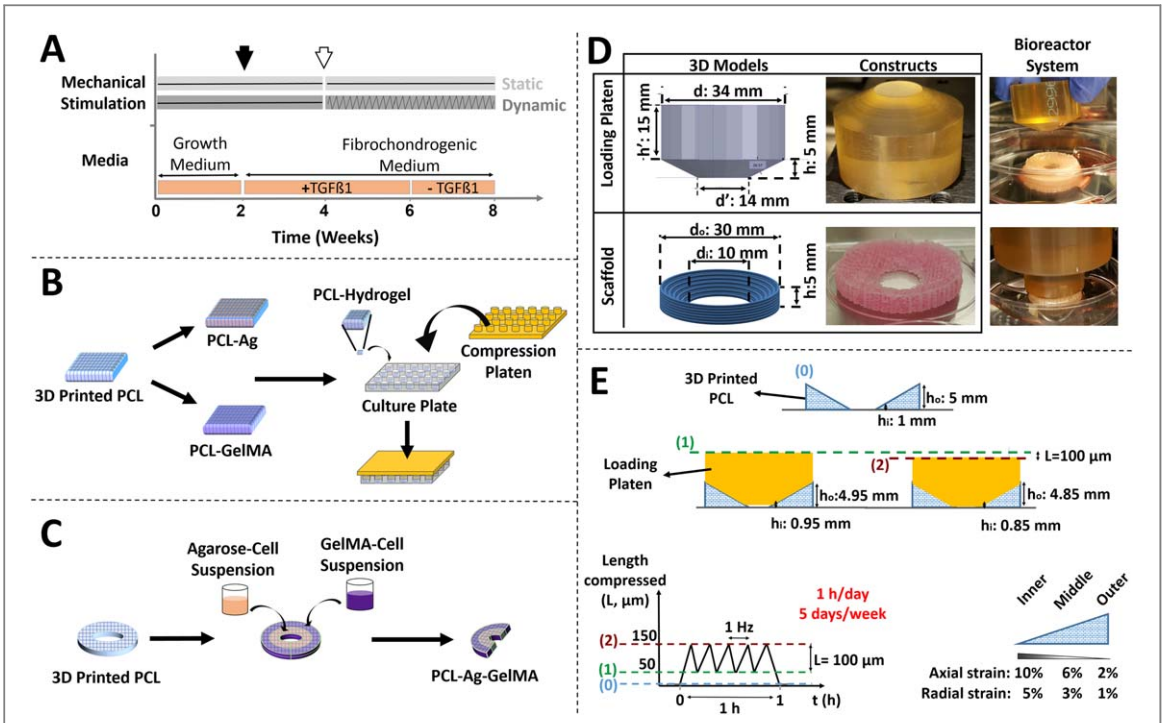

Figure 1. Diagram showing the design of the study. (A) Time plan showing the culture conditions. Full arrowheads show the time for hydrogel incorporation, and empty arrowheads show the time when dynamic stimulation was started. (B) Preparation of square prism constructs. Constructs were subjected to dynamic compression using a polysulfone-based compression platen that fits in a 24-well plate. (C) Preparation of the meniscus shaped constructs. Constructs were impregnated with agarose (Ag) in the inner region and with GelMA in the outer region. (D) Design of the meniscus shaped constructs and the loading platen used for dynamic stimulation. (E) Meniscus shaped constructs were subjected to biaxial dynamic loading. The magnitude of the strain increased gradually from the outer region towards the inner region.

2.2.3. Cell seeding and culture

Square prism PCL scaffolds were seeded with fibrochondrocytes (passage 2) at a density of 1.3×10^5 cells/scaffold and incubated for 2 weeks in growth media to allow for cell proliferation and ECM deposition (figure 1(A)). Scaffolds were then impregnated with cell-loaded agarose (Ag, low gelling temperature, Sigma-Aldrich) and GelMA (cell densities: 7×10^6 cells ml^{-1}) at Week 2 to prepare the PCL-Ag and PCL-GelMA constructs, respectively (figure 1(B)). For PCL-Ag, fibrochondrocytes were reconstituted in 30 μl heat-sterilized Ag solution (2%, w/v in DMEM: F12 at 43 °C), and constructs were left to cool for Ag to solidify. For PCL-GelMA, fibrochondrocytes were reconstituted in 30 μl GelMA solution (6.4%, w/v in growth medium containing 1% (w/v) of the photo-initiator (Irgacure 2959, Sigma-Aldrich)), and the constructs were exposed to UV radiation (λ: 365 nm) at 0.13 mW cm^{-2} for 5 min in order for GelMA to crosslink. Hydrogel-free PCL and cell-free constructs were used as controls.

Constructs were incubated for additional six weeks in fibrochondrogenic media (growth medium containing 40 mM L-proline, 1 mM non-essential amino acids NEAA, and 50 μg ml^{-1} L-ascorbic acid 2-phosphate), with addition of TGF-β1 (10 ng ml^{-1}) and dexamethasone (100 nM) at every medium change between Weeks 2 and 6. A dynamic (cyclic) compression at 10% strain (superimposed on a 5% static strain) was applied between Weeks 4 and 8, at 1 Hz, for 1 h d^{-1} and 5 days/week. Constructs were dynamically stimulated in a custom-made bioreactor [26] with a polysulfone-based platen that fit in a 24-well culture plate (figure 1(B)).

The meniscus shaped constructs were prepared similarly. PCL scaffolds were seeded with fibrochondrocytes (density: 2×10^6 cells/scaffold), incubated for 2 weeks, impregnated with cell-loaded Ag (200 μl, 7×10^6 cells ml^{-1}) in the inner region and cooled to set Ag (figure 1(C)). The constructs were then impregnated with cell-loaded GelMA (1 ml, 7×10^6 cells ml^{-1}) in the outer region (PCL-Ag-GelMA) and exposed to UV to crosslink GelMA. A specially designed loading platen that fit on the constructs and achieved biaxial mechanical stimulation was used (figure 1(D)).

At physiological conditions, the outer region of the native meniscus is subject to a 1%–5% axial (compressive) strain and a 0%–1% radial (tensile) strain [6]. The inner region undergoes a 10%–15% axial strain and a 4%–5% radial strain. Hence, we targeted a dynamic biaxial strain that increased in magnitude from the outer region (2% axial strain and 1% radial strain) towards the inner region (10% axial strain and 5% radial strain) (figure 1(E)).

2.3. Microscopic evaluation

Cell-free constructs were visualized using a stereomicroscope (Olympus, Japan). Samples were also sputter-coated with Au/Pd and examined using a scanning electron microscope (FEI Quanta, USA) under high vacuum. Strand diameter, pore size and porosity of the PCL scaffolds were measured using ImageJ software (NIH, USA).

2.4. Mechanical testing

Cell-free constructs ($n = 5$) were incubated in PBS for 24 h and tested under compressive or tensile load using CellScale mechanical tester (Univert, Canada) equipped with a 10 N load cell. Unconfined compressive testing was performed on the square prism samples at a displacement rate of 1 mm min^{-1}. Tensile testing was performed on the rectangular prism samples at a displacement rate of 1 mm min^{-1} and with a gauge length of 10 mm according to ASTM D882-00. The compressive (E^*) and tensile (E) moduli of the constructs were calculated from the elastic region of the stress-strain curves.

2.5. Cell viability

Cell viability was assessed using Live/Dead^{TM} assay (Thermo Fisher Scientific). Samples were removed from culture at Week 6, stained in a solution containing Calcein-AM (2 μM in PBS) (live cells, green) and ethidium homodimer (EthD)−1 (4 μM) (dead cells, red) for 30 min, and examined using a confocal laser scanning microscope (CLSM) (Nikon, Japan). Samples were scanned down to thicknesses of 250 and 100 μm for 4× ($n = 40$ images) and 10× ($n = 50$ images) objectives, respectively, to obtain z-stack images. These images ($n \geqslant 3$) were split into channels (converted to 8 bit images), the number of cells in each channel was counted using the ImageJ software, and cell viability was calculated.

2.6. Biochemical assays

Samples ($n = 6$) were removed from culture media at various time points, lyophilized, and digested overnight at 60 °C in papain solution (125 U ml^{-1}) (Sigma-Aldrich). DNA, sulfated glycosaminoglycan (sGAG), and hydroxyproline contents of the samples were determined with PicoGreen, dimethylmethylene blue (DMMB), and orthohydroxyproline (OHP) assays, respectively, as described previously [2]. Hydroxyproline contents were converted to collagen contents using a collagen to OHP weight ratio of 7.64 [27].

2.7. Immunofluorescence

Constructs were removed from culture medium at Weeks 6 and 8, fixed in paraformaldehyde (4%), treated with Triton X-100 (0.1%), and incubated for 30 min in 1% bovine serum albumin (BSA) solution. Samples were incubated overnight at 4 °C in mouse primary antibodies against type I (COL 1) (Sigma-Aldrich) (dilution = 1:100) or type II collagen (COL 2) (Thermo Fisher Scientific) (dilution = 1:100), and for 1 h at 37 °C in secondary antibodies (donkey anti-mouse antibodies labeled with Alexa fluor 488) (Abcam, USA). Samples were then incubated in rhodamine-phalloidin (Thermo Fisher Scientific) (dilution = 1:100) for 1 h and in DAPI (Sigma-Aldrich) for 5 min at room temperature, and examined under CLSM. Samples were scanned to thicknesses of 250 μm for the 4× ($n = 40$ images) objective and 40 μm for the 20× objective ($n = 40$), and z-stack images were created.

COL 1 and COL 2 signal intensities of the z-stack images ($n \geqslant 2$) were quantified using ImageJ. This was done by measuring the signal intensity of the green channel after manually reducing the fluorescence intensity so that no background fluorescence is visible. CLSM images of the square prism constructs were converted to 8 bit and the integrated densities (at green channels) or plot profiles along a straight line in radial direction (from the inner region towards the outer) were estimated.

2.8. Statistical analyses

Statistical analyses were performed using SPSS 23 (IBM, USA). One-way ANOVA was performed for the mechanical properties, and the DNA, GAG and collagen contents (results at Weeks 4, 6, and 8 were compared with those at Week 2). Two-way ANOVA (independent variables: material and loading regimen) was performed to compare cell viability, net GAG and collagen produced, and COL 1 and COL 2 fluorescence intensities. Three-way ANOVA was performed when comparing GAG and collagen production to test whether the independent variables (material, loading regimen, and use of growth factor) had interaction. Tukey and Dunnett's T3 post-hoc tests were performed for sample groups having equal and unequal variance, respectively. Difference between variances was tested using Levene's test. Unpaired student t-test was performed to compare static and dynamic samples. Data are presented as the mean ± standard deviation. Significance level was $\alpha < 0.05$.

3. Results

3.1. Macroscopic and microscopic evaluation

PCL scaffolds had smooth and straight strands (figures 2(A) and (B)). The average strand diameter was 211 ± 18 μm, and the pore size was 751 ± 43 μm in xy-direction and 97 ± 40 μm in z-direction. The porosity of the scaffolds was 68% ± 7%. For the PCL/hydrogel constructs, the pores of the scaffolds were almost completely filled with the hydrogels (figure 2(B)).

3.2. Mechanical properties

Compressive moduli of PCL, PCL-Ag, and PCL-GelMA were 11.5 ± 1.1, 8.4 ± 2.2, and 10.0 ± 1.9 MPa,

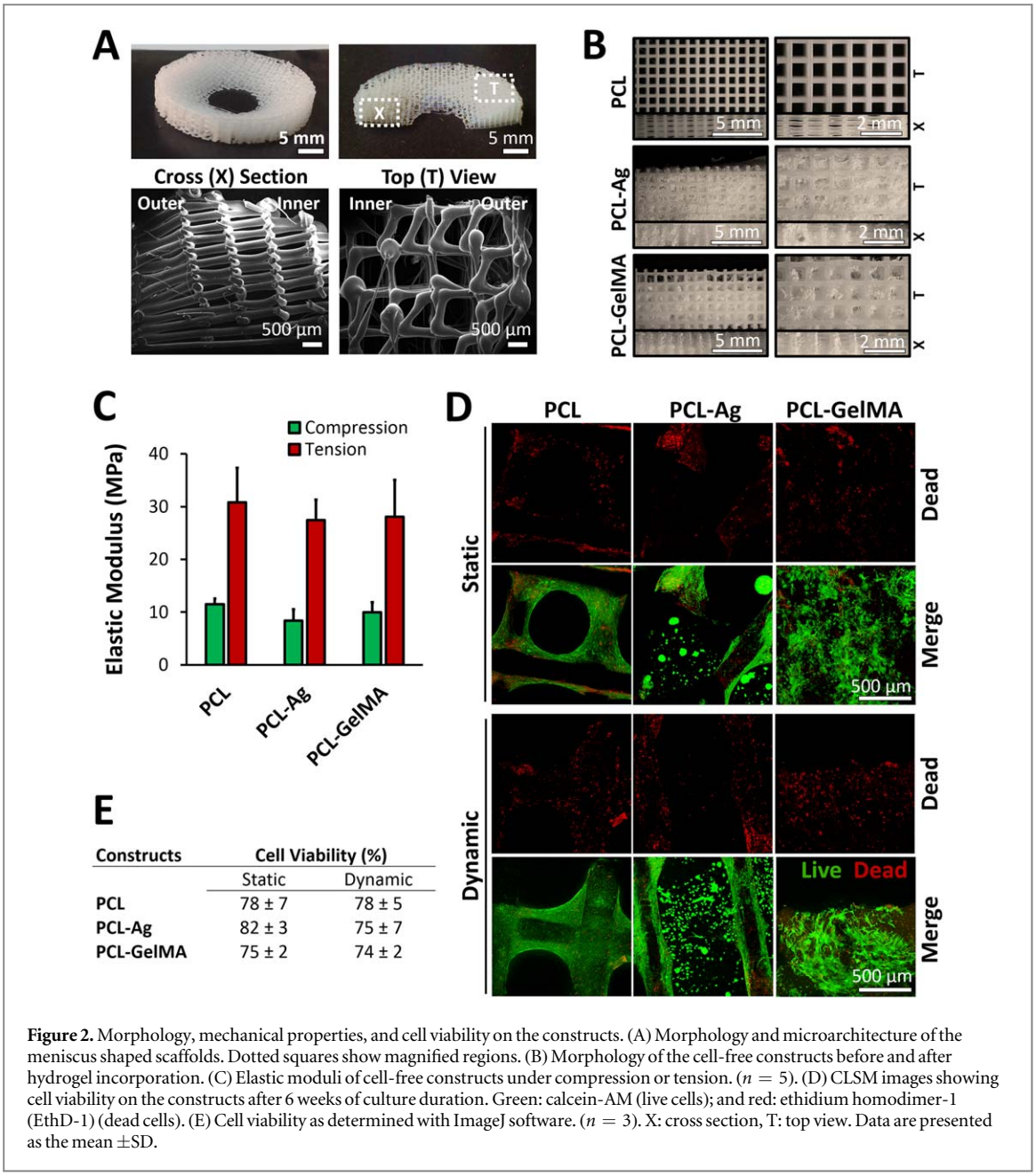

Figure 2. Morphology, mechanical properties, and cell viability on the constructs. (A) Morphology and microarchitecture of the meniscus shaped scaffolds. Dotted squares show magnified regions. (B) Morphology of the cell-free constructs before and after hydrogel incorporation. (C) Elastic moduli of cell-free constructs under compression or tension. ($n = 5$). (D) CLSM images showing cell viability on the constructs after 6 weeks of culture duration. Green: calcein-AM (live cells); and red: ethidium homodimer-1 (EthD-1) (dead cells). (E) Cell viability as determined with ImageJ software. ($n = 3$). X: cross section, T: top view. Data are presented as the mean ±SD.

respectively (figure 2(C)). Tensile moduli of the constructs were 30.8 ± 6.6, 27.4 ± 3.8, and 28.1 ± 6.9 MPa, respectively. Incorporation of Ag and GelMA hydrogels slightly, but not significantly, reduced mechanical properties of the constructs.

3.3. Cell viability

Live/dead assay revealed high cell viability on the constructs at Week 6 (figure 2(D)). Cells on PCL were elongated, those on Ag were round, and those on GelMA were dendritic. Quantitative analysis showed that cell viability on the constructs was in the range of 74%–82% (figure 2(E)). Dynamic compression at 10% strain had no significant effect on cell viability.

DNA content, which represents the cell number, is given as the relative DNA content at a specific time point with respect to (wrt) that at Week 2. Relative DNA content remained relatively constant on PCL-Ag throughout the culture period, and it increased significantly on PCL and PCL-GelMA after Week 2 ($p < 0.05$) (figure 3(A)). The highest increase in DNA content was obtained with PCL-GelMA (60%–80% increase by Weeks 6 and 8), showing a high rate of cell proliferation on this construct. Dynamic compression decreased the DNA content of PCL by 18% ($p < 0.05$), increased that of PCL-Ag by 34% ($p < 0.01$), and did not change that of PCL-GelMA. This indicated that hydrogels protected the cells against the damage caused by dynamic compression.

3.4. Sulfated GAG content

Addition of hydrogels increased the production of sulfated GAGs, and the highest production was obtained with PCL-Ag (figure 3(B)). Dry weight-normalized

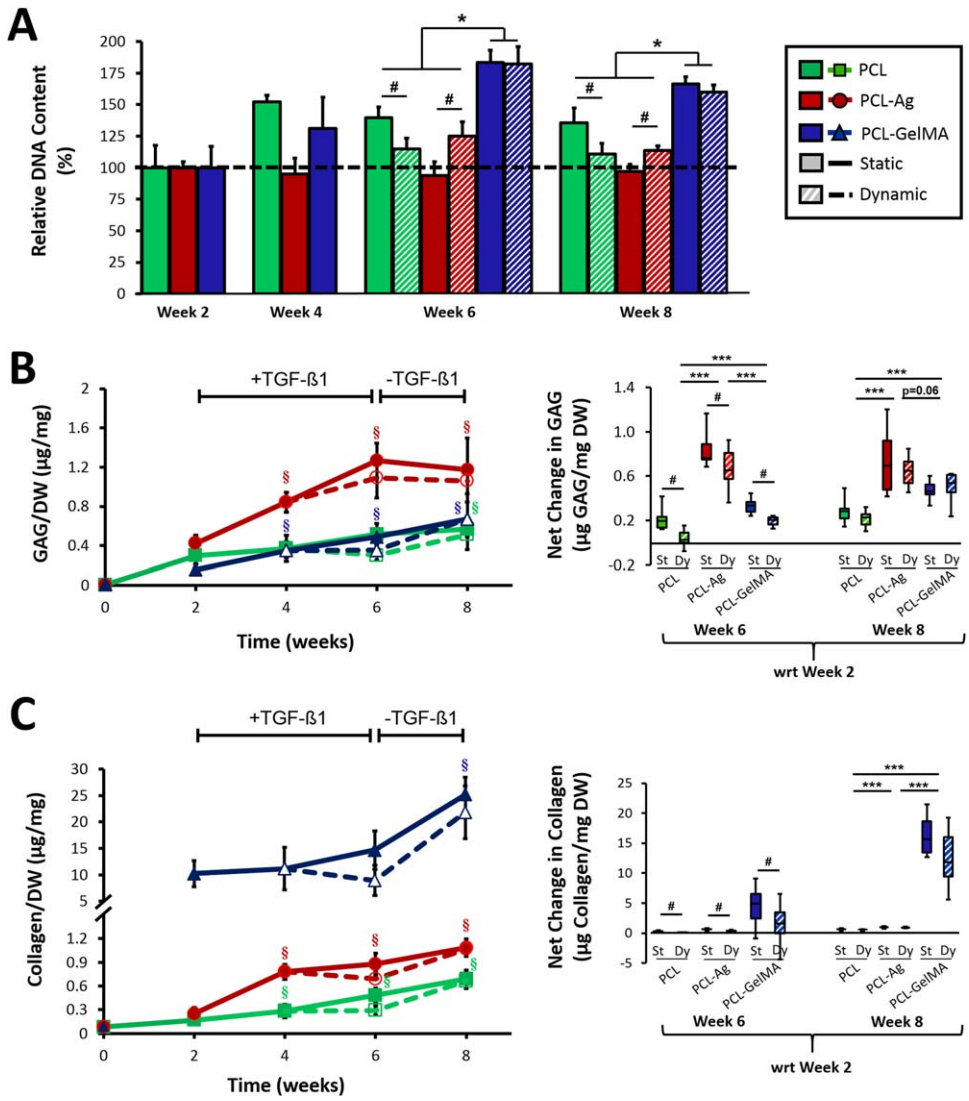

Figure 3. Effects of hydrogels, dynamic stimulation, and TGF-β1 on the biochemical composition of the constructs. (A) Relative DNA contents (%) with respect to (wrt) Week 2 (dashed line). ($n = 6$). (B) Sulfated GAG contents (left), and the net change wrt Week 2 (right). ($n = 6$). (C) Collagen contents (left), and the net change wrt Week 2 (right) ($n = 6$). Static: St, continuous lines, full columns; and Dynamic: Dy, dashed lines, patterned columns. Hydrogel incorporation: Week 2, start of dynamic stimulation: Week 4[§#*].

GAG contents increased over time in all the constructs incubated under static conditions, and this increase was significant for PCL-Ag (2–3 folds) and PCL-GelMA (2–4 folds) after Week 2 ($p < 0.05$) (figure 3(B), left). Dynamic compression significantly reduced GAG contents between Weeks 4 and 6, during which TGF-β1 was present ($p < 0.05$), and it increased GAG contents after Week 6, during which TGF-β1 was not present. On the other hand, removal of TGF-β1 (after Weeks 6 and 8) reduced GAG production only on PCL-Ag (by 3%–8%), regardless of whether constructs were dynamically compressed. The net GAG production was the GAG contents at Weeks 6 and 8 wrt Week 2. The highest GAG production after hydrogel addition was observed on PCL-Ag (figure 3(B), right). In the presence of TGF-β1 (Week 6 results), dynamic compression lowered the GAG production by 15% ($p < 0.05$), but when TGF-β1 was removed from culture media (Week 8 results), the difference between GAG production of static and dynamic samples was eliminated. Similar results were observed when GAG contents were normalized to DNA (figure S1(A) is available online at stacks.iop.org/BF/11/025002/mmedia).

3.5. Collagen content

Addition of hydrogels increased the collagen production, and the highest increase was with PCL-GelMA (figure 3(C)). Under static conditions, collagen contents increased significantly over time ($p < 0.05$) (figure 3(C), left). In the presence of TGF-β1 (between Weeks 4 and 6), collagen production decreased upon

§ Significant difference between results of a particular construct at a particular time point wrt Week 2.

Significant difference between the St and Dy groups of a particular construct at a particular time point.

* Significant difference between the constructs at a particular time point. *p 0.05, ***p 0.001.

dynamic compression, and in the absence of it (between Weeks 6 and 8), collagen production increased. The net collagen production was the collagen contents at Weeks 6 and 8 wrt Week 2. The net collagen production on constructs was very low in the presence of TGF-β1 (between Weeks 2 and 6), and it dropped further upon dynamic compression ($p < 0.05$) (figure 3(C)), right). In the absence of TGF-β1 (after Week 6), dynamic compression increased the production of collagen. At Week 8, the highest collagen content was obtained with PCL-GelMA ($p < 0.001$). Removal of TGF-β1 from culture media resulted in a significant increase in collagen production on PCL-GelMA (three-fold increase) ($p < 0.05$). Again similar results were observed when collagen contents were normalized to DNA (figure S1(B)).

Statistical analyses using three-way ANOVA revealed that there was a significant interaction between the material type, the use of TGF-β1, and the loading regimen ($p < 0.01$). This meant that each material reacted differently to dynamic compression and TGF-β1. Presence of TGF-β1 significantly increased GAG production on PCL-Ag and decreased collagen production on PCL-GelMA (figures S1(C) and S1(D)). However, when dynamic compression was applied in the presence of TGF-β1, GAG and collagen production were influenced negatively, independent of the material. For PCL-Ag, the highest rate of GAG production was obtained in the presence of TGF-β1 and absence of dynamic loading (figure S1(C)). Regardless of the material, the highest collagen production was obtained when dynamic stimulation was applied in the absence of TGF-β1 (figure S1(D)). The material type was the most effective factor to determine the level of ECM produced on constructs.

3.6. Immunofluorescence

3.6.1. The effect of hydrogels and dynamic compression on collagen deposition.

The whole constructs were immunostained for COL 1 and COL 2. Collagen deposition on the surface of constructs (within 250 μm depth) was evaluated using a CLSM. COL 1 staining on PCL was more intense than COL 2 at Weeks 6 (figure S2) and 8 (figure 4(A)). Long and continuous collagen fibers were produced and they were aligned along the PCL strands (figure S3). When Ag was introduced, the intensity of collagen staining was increased (figure 4(B)). COL 1 staining intensities were similar in Ag and on PCL, but COL 2 intensity was more intense in Ag. The collagen produced on PCL was fibrous, while that produced on Ag was globular.

The most intense collagen staining was observed on PCL-GelMA, where COL 1 staining was more intense than COL 2 (figure 4(C)). In fact, a fibrous network of COL 1 was visible on the GelMA side of the constructs (figure S3). Collagen staining intensities were similar on the static (left) and dynamic (right) constructs.

Quantitative analysis of the CLSM images showed that presence of hydrogels in the constructs enhanced the collagen production (figure 5). The most intense collagen (mainly COL 1) staining was obtained with PCL-GelMA. COL 1 staining intensity increased after the addition of GelMA, and this increase was significant at Week 8 ($p < 0.001$) (figure 5(A)). COL 2 staining intensity also increased with the addition of hydrogels (figure 5(B)). Dynamic compression increased the COL 2 production on PCL-GelMA by 40% ($p < 0.05$ at Week 8), and had no effect on the other materials.

At Week 6, the ratio of COL 2 to total collagen was higher on PCL-Ag (around 50% of total collagen) than on PCL (around 40%) and PCL-GelMA (around 45%) (figure 5(C)). Dynamic compression had no effect on this ratio. Removal of TGF-β1 after Week 6 resulted in a decreased COL 2 ratio in all constructs, but dynamically compressing the constructs resulted in increased COL 2 ratio (Week 8).

3.6.2. Collagen deposition on meniscus shaped constructs

The meniscus shaped constructs were impregnated with Ag in the inner region and with GelMA in the outer region. In the inner region the intensities of COL 1 and COL 2 were comparable, while in the outer region COL 1 intensity was more intense than that of COL 2 (figure 6). COL 1 was more intense on the outer region of the constructs than the inner region both in the static (figure 6(A)) and in dynamic samples (figure 6(B)), although this was partly due to autofluorescence of GelMA.

Quantitative analysis was done after eliminating the background autofluorescence. COL 1 intensity was higher in the outer region of the constructs than the inner region, while COL 2 intensity was similar in the inner and outer regions (figures 6(C) and (D)). In the inner region of the dynamically stimulated constructs, collagen intensity increased gradually towards the middle part, where samples received dynamic stimulation at a medium level of strain (figure 6(D)). When compared to the static samples, dynamically stimulated samples deposited higher COL 1 especially in the outer region (figures 6(C) and (D)). Under static conditions, the ratio of COL 2 to total collagen was higher in the inner region (50%) than the outer region (40%). Upon dynamic stimulation, this ratio increased further in the inner region (60%), and decreased in the outer region (30%). The interfaces between PCL and hydrogels or between Ag and GelMA (figures S3 and S4) showed that the hydrogels were well incorporated in the PCL structure and they also integrated well with each other.

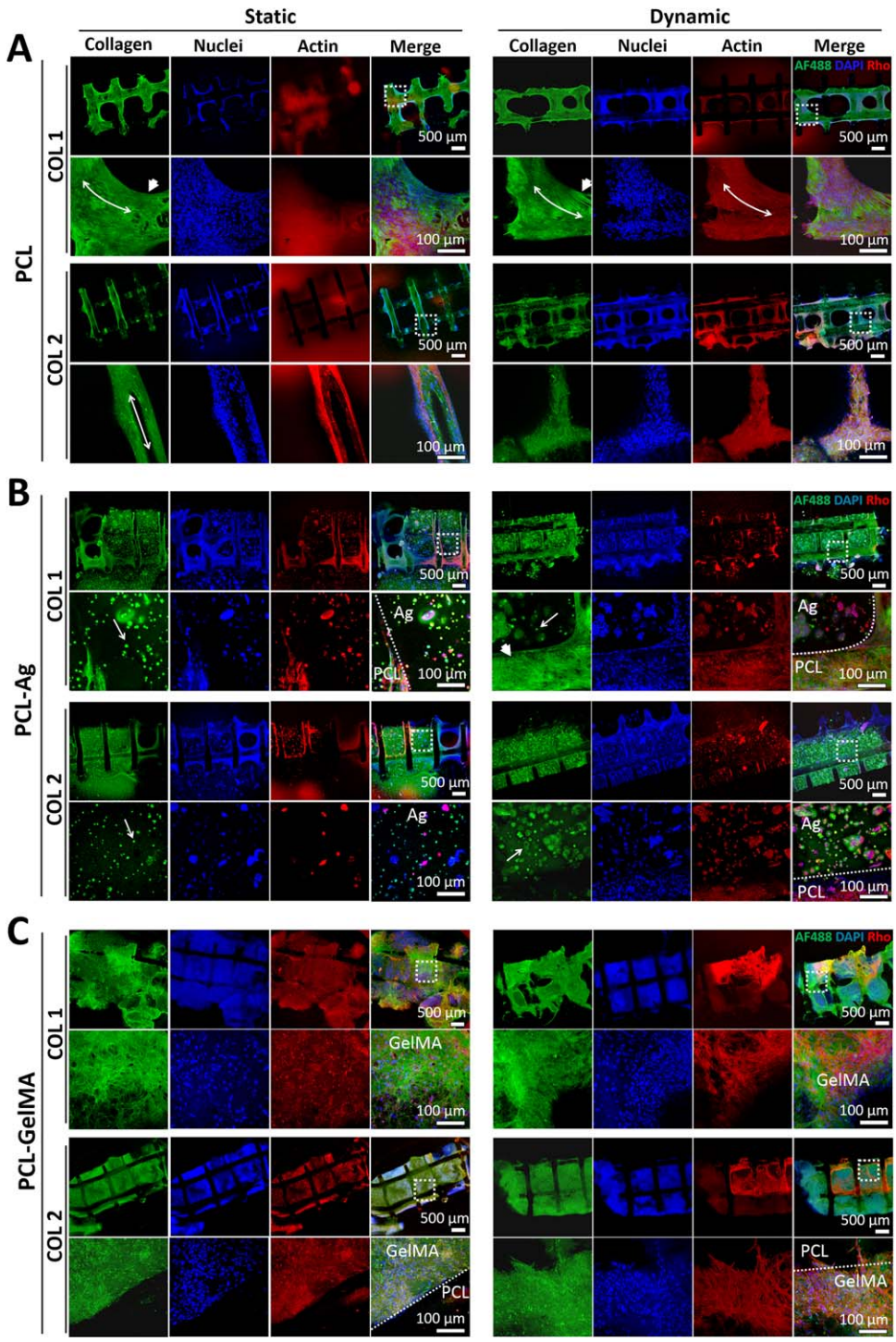

Figure 4. Immunofluorescence images showing collagen type I (COL 1) and II (COL 2) deposition on the constructs after 8 weeks of cultivation. (A) PCL, (B) PCL-Ag, and (C) PCL-GelMA. Green: Alexa fluor 488 (collagen), blue: DAPI (nuclei), and red: rhodamine-phalloidin (actin). Dotted squares: magnified regions. Dotted lines: borders between PCL and hydrogels. Arrowheads: fibrous collagen, arrows: globular collagen, double-sided arrows: alignment of collagen or cells.

4. Discussion

In this study, we aimed to produce a PCL/hydrogel based construct closely mimicking the biochemical organization of the native meniscus. This was achieved by printing a meniscus shaped PCL scaffold and impregnating its inner region with Ag hydrogel and its outer region with GelMA hydrogel. After 8 weeks of incubation with porcine fibrochondrocytes, the inner region of the constructs exhibited high levels of chondrogenic ECM components, GAGs and COL 2, and the outer region exhibited a high level of the fibrous component, COL 1 (figure 6). Hydrogels also protected the cells from the mechanical damage caused by dynamic compression (figure 3). Our construct could be used as a candidate scaffold for total meniscal replacement, because it exhibits appropriate mechanical properties, high cell viability, and

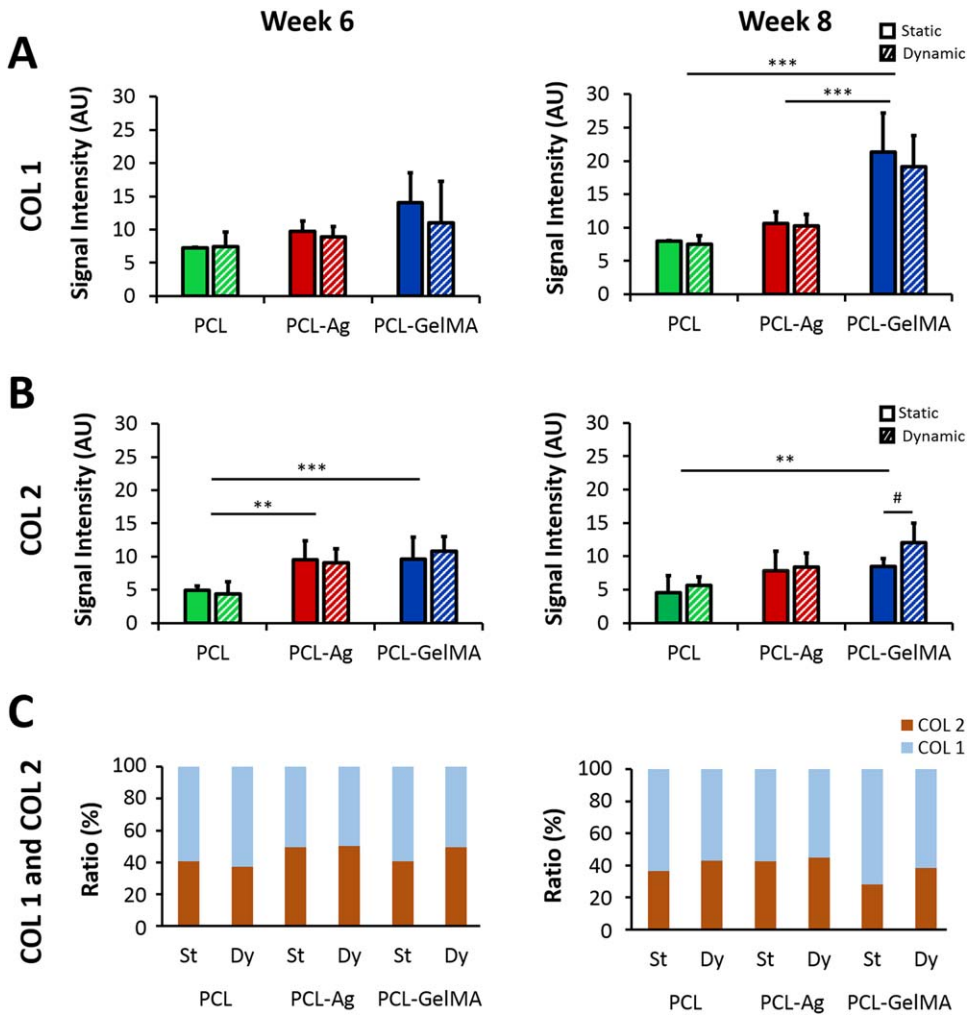

Figure 5. Quantitative analysis of the immunofluorescence images using ImageJ showing the effect of hydrogel incorporation and dynamic stimulation on collagen production. Intensities of (A) COL 1 and (B) COL 2. (C) The ratio of COL 2 to total collagen in the constructs at Weeks 6 and 8[#*].

biochemical composition closely mimicking that of the meniscus.

3D printed PCL-based scaffolds have been proposed for meniscus regeneration by many researchers [16–20]. Most of these researchers have not intended to mimic the biochemical composition of the meniscus. The only study in which a zone-specific biochemical composition was targeted involved the use of TGF-β3—loaded PLGA microspheres in the inner region of the 3D printed PCL to induce cartilaginous phenotype and CTGF—loaded microspheres in the outer region to induce fibrous phenotype [20]. However, the PCL scaffolds led to degenerated articular cartilage 12 weeks post implantation in rabbit [19] and sheep [20] models, due to friction. In our construct, we impregnated our 3D printed PCL scaffolds with hydrogels to protect the articular cartilage from any mechanical damage caused as a result of friction. Hydrogels softened the surface of PCL (figure 2), protected the cells from damage under a physiologically relevant dynamic load (figure 3), and increased ECM production significantly compared to hydrogel-free scaffolds (figures 3–5). Daly and colleagues [16] also combined PCL scaffolds with one of alginate, agarose, methacrylated polyethylene glycol (PEGMA) and GelMA hydrogels for possible use in fibrocartilage regeneration, but our design includes the use of two different hydrogels in the different regions of the constructs to create a zone-specific biochemical composition resembling that of the meniscus. The advantages of our approach are that, first, it involves cell seeding on PCL and incubation for 2 weeks, which would result in elongated cells and aligned collagen fibers. Second, it involves incorporation of cell-loaded hydrogels to create zonal variation between the different regions of the construct. Third, the hydrogels could protect the cells as well as the hyaline cartilage against dynamic load.

The elastic moduli of the cell-free constructs were around 10 MPa under compressive load and 30 MPa

[#] Significant difference between the static and dynamic groups of a particular construct.

[*] Significant difference between constructs. [**]p 0.01, [***]p 0.001.

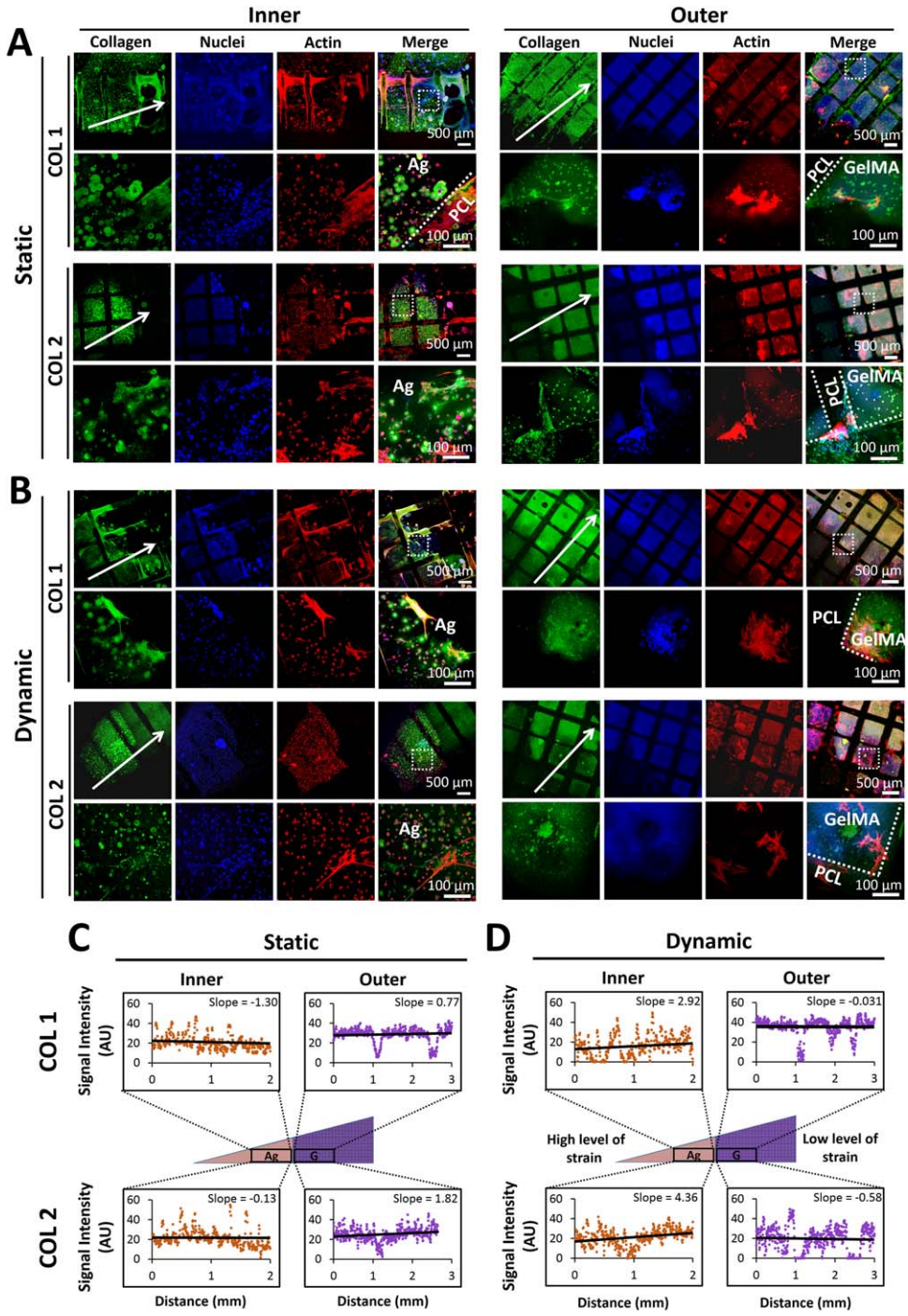

Figure 6. Immunostaining of the meniscus shaped constructs after 8 weeks of incubation. Representative CLSM images of the constructs incubated under (A) static, and (B) dynamic conditions. Green: Alexa fluor 488 (collagen), blue: DAPI (nuclei), and red: rhodamine-phalloidin (actin). Dotted squares: magnified regions. Dotted lines: borders between the hydrogels and PCL. Arrows show the direction from the inner region of constructs to the outer region. Quantitative analysis showing the collagen staining intensities on the constructs incubated under (C) static, and (D) dynamic conditions. Histograms show the change in collagen signal intensity along the arrows on the CLSM images. Ag: agarose-impregnated, G: GelMA-impregnated regions. Biaxial dynamic stimulation was applied at a high strain in the inner region and at a low strain in the outer region. A positive slope shows an increase in collagen intensity towards the outer region, and a negative slope shows a decrease.

under tensile load; addition of hydrogels had almost no effect on the mechanical properties of the scaffolds (figure 2(C)). Compressive modulus of the constructs was higher than the native porcine (1–5 MPa) [28] and human (0.3–2 MPa) [29, 30] menisci. Tensile modulus, however, was significantly lower than the native porcine (113–142 MPa) [31] and human menisci (78–125 MPa) [32] measured in circumferential direction, and comparable with that of human meniscus measured in radial direction (4–20 MPa). Our results were obtained from the cell-free constructs, and the mechanical properties were expected to get closer to those of native tissue in the presence of cells or after implantation in animal models [11, 19, 33]. In

addition, these results are comparable with those of other 3D printed PCL scaffolds intended for use in meniscal regeneration, which have compressive modulus in the range 10–54 MPa and tensile modulus in the range 40–80 MPa [17–20]. It would be possible to increase tensile modulus of our constructs by changing the printing parameters such as shortening the strand-to-strand distance or increasing the strand diameter [14, 17]. However, this would also increase the compressive modulus, further diverging our results from the native meniscus values.

The PCL scaffolds were intentionally printed with large pores, allowing for easy infiltration of the hydrogels, and transport of oxygen and nutrients. Quantitative measurements showed that the pore width was about 750 μm in *xy*-direction and 100 μm in *z*-direction, large enough to facilitate these. In fact, the pores of our scaffolds were filled completely with hydrogels and cells were uniformly distributed throughout the hydrogel-impregnated constructs (figure 2). Although the optimal pore size for meniscal regeneration is between 150 and 500 μm [34], there is the possibility of skin layer formation at the surface of scaffolds with pores of below 120 μm in diameter, which could block tissue infiltration [35], and nutrient and oxygen transport (limited to a 200 μm distance from the blood vessels) [36]. Thus, the large pores in our constructs would be useful for cell and tissue infiltration, and cell viability after implantation.

Cell viability was similar on all the constructs (around 80%) (figures 2(D) and (E)). However, the highest increase in DNA content (corresponding to cell number) was on PCL-GelMA (around 75% increase) (figure 3(A)), probably due to presence of biologic recognition sites such as arginine-glycine-aspartic acid (RGD) sequences on gelatin [37]. Although most of the cells on the Ag part of PCL-Ag were viable (figure 3(C)), there was almost no increase in the cell number on this construct over time (figure 3(A)), probably because Ag lacks the biochemical cues that promote cell adhesion, and is highly hydrophilic and repels cells from binding [38]. On PCL, cell proliferation was high during the first 4 weeks of culture, probably because it has an appropriate stiffness and hydrophobicity supporting spreading and proliferation of the fibrochondrocytes [2, 39]. However, cell viability was low on the PCL strands after addition of hydrogels (figure 2(D)), probably because of the extensively increased number of cells on the PCL strands, which depleted the nutrients and oxygen. Similarly, cell viability was reported to decrease upon introduction of PCL to Ag (from 90% to 80%) or GelMA (from 82% to 78%) [16], which supported our finding.

Upon dynamic compression, cell number (reported as DNA content) decreased on PCL scaffolds, but no decrease was observed on PCL/hydrogel constructs (figure 3(A)). In order to create a dynamic compression at 10% strain, a large stress (up to 1.7 MPa) was applied on the PCL scaffolds. This high stress probably led to cell damage on PCL scaffolds and decreased the cell number. However, when hydrogels were present, the cells were not directly exposed to the mechanical load, and thus were protected from its harmful effects. While the DNA content of PCL-Ag increased upon dynamic loading (figure 3(A)), the ratio of dead cells on these constructs did not change (figure 2(E)), showing that the high DNA content is not due to the dead cells retained in the hydrogels. Others also reported that the DNA content of hydrogels decreased upon dynamic compression at 10% [2, 40] and 15% [41] strain, which also showed that dead cells are not normally retained in the hydrogels but are released to culture media. These results indicate that hydrogels would also protect the cartilage from the mechanical damage after implantation. In fact, intra-articular injection of GelMA-based hydrogels was reported to significantly reduce cartilage degeneration as compared to GelMA-untreated controls in anterior cruciate ligament-transected mice [42]. Still, the effect of the hydrogels on cartilage degeneration should be tested in a large animal model before any decisive conclusions are reached.

PCL scaffolds exhibited low levels of collagen, which was mainly COL 1 (figures 3–6). Introduction of hydrogels to PCL scaffolds significantly enhanced GAG and collagen levels; there was increased production of GAGs and COL 2 on the Ag-impregnated constructs, and increased production of total collagen (especially COL 1) on the GelMA-impregnated constructs. This could be linked to the different levels of cell-material interactions. The stiff PCL directs cells to proliferation instead of ECM production [2, 39]. The soft and non-bioactive Ag leads to reduced cell adhesion and round cell morphology, which directs cells to chondrogenic phenotype. GelMA, on the other hand, has the RGD sequences and enhances cell adhesion and spreading, and promotes fibrogenic phenotype. In fact, inhibition of focal adhesion kinases of nucleus pulposus cells embedded in GelMA was reported to lead to a more rounded cell morphology and enhanced chondrogenesis [43]. Similar to our results, Daly and colleagues reported higher COL 1 production in GelMA and higher COL 2 production in Ag hydrogels [16].

Because of the controversial reports regarding the combined effects of TGF-β and mechanical loading on cell behavior [44], we chose to add TGF-β1 at the first half of the loading period (Weeks 4–6) and remove it during the second half (Weeks 6-8) to investigate its effect on meniscal ECM production in the absence and presence of dynamic loading. Presence of TGF-β1 increased the GAG production on PCL-Ag, and decreased the collagen production on PCL-GelMA (figures 3 and S1). Agarose is chondrogenic [2], and thus TGF-β1, which is also chondrogenic [45], augments GAG production on this hydrogel. On the other hand, GelMA is fibrogenic, and thus TGF-β1

reduces collagen production on this hydrogel. Similar to our finding, TGF-β1 was reported to be more effective than dynamic compression in increasing the GAG and collagen production in Ag hydrogels [46].

On the other hand, we showed that dynamic compression at 10% strain resulted in increased ECM production only in the absence of TGF-β1. ECM production has been reported to increase upon dynamic compression at 5% [47], 10% [40, 48, 49], 15% [41], and 20% strain levels [50]. But when TGF-β and dynamic compression were applied simultaneously, ECM production was reported to decrease [46, 51]. Hence, we concluded that TGF-β1 and dynamic compression should be applied individually, but not simultaneously. When a cartilage-like tissue is targeted TGF-β1 and Ag could be used, and when a fibrous tissue is desired GelMA could be used but without TGF-β1. For engineering of the meniscus *in vitro*, the inner region of the constructs could be impregnated with the TGF-β1—embedded Ag, and dynamic stimulation could be applied only on the GelMA-impregnated outer region. In a potential clinical application, mechanical stimulation would be avoided during the non-active recovery phase after surgery to ensure complete release of TGF-β1 before mechanical stimulation is applied through walking.

Finally, meniscus shaped PCL scaffolds were seeded with cells, incubated for 2 weeks, and impregnated with cell-loaded Ag in the inner region and with cell-loaded GelMA in the outer region. The constructs were subjected to dynamic load that increased in magnitude from the outer region towards the inner region by the help of a specially designed loading platen (figure 1). Under static conditions, the outer portion of the constructs exhibited higher COL 1 production than the inner portion, but COL 2 production was similar in the two regions (figure 6). Thus, COL 2 ratio was higher in the inner region (50% of total collagen) than the outer (40%). When the constructs were subjected to physiologically relevant biaxial dynamic stimulation, COL 1 deposition increased in the outer region, and COL 2 increased in the inner region. But the collagen level depended on the magnitude of dynamic compression. Collagen intensity increased from the inner region of the constructs, where a high level of dynamic strain was applied (10% axial strain and 5% radial strain), towards the middle region, where strain was at medium level (6% axial strain and 3% radial strain). Upon dynamic stimulation, COL 2 ratio in the inner region increased to 60%, and COL 1 ratio in the outer region increased to 70%. This biochemical composition is very close to that of the native meniscus, at which COL 1 constitutes 80% of the collagen in the outer region and COL 2 constitutes 60% of that in the inner region [1].

5. Conclusions

We have shown that a meniscal construct that closely mimics the biochemical composition of the native tissue could be engineered by using Ag and GelMA hydrogels in the inner and outer regions of the 3D printed PCL scaffolds, respectively. Ag enhances GAG and COL 2 production, and is suitable for use in regeneration of the inner region of the meniscus. GelMA enhances collagen (especially COL 1) production and is suitable for the outer region. TGF-β1 increases GAG production rate on PCL-Ag and decreases collagen production rate on PCL-GelMA, while dynamic stimulation increases GAG and collagen production rates on all the constructs but only when applied in the absence of TGF-β1. Biaxial mechanical stimulation of the meniscus shaped constructs further increases COL 2 deposition in the inner region and COL 1 deposition in the outer region. The use of hydrogels not only enhances ECM production, but also protects the cells from mechanical damage under physiologically relevant loading environment. We concluded that 3D printed PCL-based, tissue engineered scaffolds should be dynamically stimulated at medial strain levels (3% radial strain and 6% axial strain) in order to optimally enhance ECM deposition, and TGF-β1 should be used only with Ag-based constructs and without dynamic compression. This study is significant in showing that hydrogels could be used to create tissue constructs with biochemical composition similar to that of native tissues. Our loading platen which enables physiologically relevant dynamic stimulation of the meniscus constructs could serve as a valuable tool to evaluate the constructs before implantation into animals. Our construct perform well under pysiologically relevant loading environment, and could serve as a functional and mechanically stable substitute for use in partial or total replacement of the meniscus. Future work will involve co-printing of the hydrogels with PCL to create a more automated, translational approach, and testing of these constructs in a pig model.

Acknowledgments

Authors declare that there is no conflict of interests. This project was supported by BIOMATEN, METU through BAP-08-11-2016-022 and the US Department of Veterans Affairs Rehabilitation Research and Development Service through 5IK2RX000760. GB was supported by TUBITAK through BİDEB 2214/A. The RIH Core Research Laboratories and Ginny Hovanesian are acknowledged for their assistance with histology and imaging.

ORCID iDs

Gokhan Bahcecioglu https://orcid.org/0000-0002-6228-4745
Nesrin Hasirci https://orcid.org/0000-0002-4497-019
Bahar Bilgen https://orcid.org/0000-0002-7395-2315
Vasif Hasirci https://orcid.org/0000-0002-3698-8861

References

[1] Cheung H S 1987 *Connective Tissue Res.* **16** 343–56
[2] Bahcecioglu G, Hasirci N, Bilgen B and Hasirci V 2019 *Int. J. Biol. Macromol.* **122** 1152–62
[3] Sanchez-Adams J, Willard V P and Athanasiou K A 2011 *J. Appl. Physiol.* **111** 1590–6
[4] Paul J P 1976 *Proc. R. Soc.* B **192** 163–72
[5] Shrive N G, O'Connor J J and Goodfellow J W 1978 *Clin. Orthop. Relat. Res.* **131** 279–87
[6] Freutel M, Seitz A M, Galbusera F, Bornstedt A, Rasche V, Knothe Tate M L, Ignatius A and Dürselen L 2014 *J. Magn. Reson. Imaging* **40** 1181–8
[7] Bilgen B, Jayasuriya C T and Owens B D 2018 *Adv. Healthcare Mater.* **7** e1701407
[8] Mandal B B, Park S H, Gil E S and Kaplan D L 2011 *Biomaterials* **32** 639–51
[9] Bahcecioglu G, Buyuksungur A, Kiziltay A, Hasirci N and Hasirci V 2014 *J. Bioact. Compat. Pol.* **29** 235–53
[10] Halili A N, Hasirci N and Hasirci V 2014 *J. Mater. Sci., Mater. Med.* **25** 1195–209
[11] Baker B M, Shah R P, Huang A H and Mauck R L 2011 *Tissue Eng.* **17** 1445–55
[12] Gao S, Guo W, Chen M, Yuan Z, Wang M, Zhang Y, Liu S, Xi T and Guo Q 2017 *J. Mater. Chem.* B **5** 2273–85
[13] Visser J, Peters B, Burger T J, Boomstra J, Dhert W J, Melchels F P and Malda J 2013 *Biofabrication* **5** 035007
[14] Buyuksungur S *et al* 2017 *Biomater. Sci.* **5** 2144–58
[15] Malikmammadov E, Endogan Tanir T, Kiziltay A, Hasirci V and Hasirci N 2018 *J. Biomat. Sci. Polym Ed.* **29** 863–93
[16] Daly A C, Critchley S E, Rencsok E M and Kelly D J 2016 *Biofabrication* **8** 045002
[17] Cengiz I F, Pitikakis M, Cesario L, Parascandolo P, Vosilla L, Viano G, Oliveira J M and Reis R L 2016 *Bioprinting* **1–2** 1–10
[18] Szojka A, Lalh K, Andrews S H J, Jomha N M, Osswald M and Adesida A 2017 *Bioprinting* **8** 1–7
[19] Zhang Z Z, Wang S J, Zhang J Y, Jiang W B, Huang A B, Qi Y S, Ding J X, Chen X S, Jiang D and Yu J K 2017 *Am. J. Sports Med.* **45** 1497–511
[20] Lee C H, Rodeo S A, Fortier L A, Lu C, Erisken C and Mao J J 2014 *Sci. Transl. Med.* **6** 266ra171
[21] Dreesmann L, Ahlers M and Schlosshauer B 2007 *Biomaterials* **28** 5536–43
[22] Lee Y, Balikov D A, Lee J B, Lee S H, Lee S H, Lee J H, Park K D and Sung H J 2017 *Int. J. Mol. Sci.* **18** E1705
[23] Kreimendahl F, Köpf M, Thiebes A L, Duarte Campos D F, Blaeser A, Schmitz-Rode T, Apel C, Jockenhoevel S and Fischer H 2017 *Tissue Eng.* C **23** 604–15
[24] Hasirci N, Kilic C, Kömez A, Bahcecioglu G and Hasirci V 2016 *Hydrogels in Regenerative Medicine Gels Handbook: Fundamentals, Properties and Applications* (*Applications of Hydrogels in Regenerative Medicine*) ed U Demirci and A Khademhosseini vol 2 (Singapore: World Scientific)
[25] Kilic Bektas C and Hasirci V 2018 *J. Tissue Eng. Regen. Med.* **12** e1899–910
[26] Bilgen B, Chu D, Stefani R and Aaron R K 2013 *J. Vis. Exp.* **74** e50387
[27] Hollander A P, Heathfield T F, Webber C, Iwata Y, Bourne R, Rorabeck C and Poole A R 1994 *J. Clin. Invest.* **93** 1722–32
[28] Yasura K *et al* 2007 *J. Orthop. Res.* **25** 884–93
[29] Chia H N and Hull M L 2008 *J. Orthop. Res.* **26** 951–6
[30] Fischenich K M, Boncella K, Lewis J T, Bailey T S and Haut Donahue T L 2017 *J. Biomed. Mater. Res.* A **105** 2722–8
[31] Abdelgaied A, Stanley M, Galfe M, Berry H, Ingham E and Fisher J 2015 *J. Biomech.* **48** 1389–96
[32] Tissakht M and Ahmed A M 1995 *J. Biomech.* **28** 411–22
[33] Han W M, Heo S J, Driscoll T P, Delucca J F, McLeod C M, Smith L J, Duncan R L, Mauck R L and Elliott D M 2016 *Nat. Mater.* **15** 477–84
[34] Klompmaker J, Jansen H W and Veth R H 1993 *Clin. Mater.* **14** 1–11
[35] Murphy C M, Haugh M G and O'Brien F J 2010 *Biomaterials* **31** 461–6
[36] Jain R K, Au P, Tam J, Duda D G and Fukumura D 2005 *Nat. Biotechnol.* **23** 821–3
[37] Liu Y and Chan-Park M B 2010 *Biomaterials* **31** 1158–70
[38] Jeuken R M, Roth A K, Peters R J, van Donkelaar C C, Thies J C, van Rhijn L W and Emans P J 2016 *Polymers* **8** 219
[39] Bahcecioglu G, Hasirci N and Hasirci V 2018 *Biomed. Mater.* **13** 035005
[40] Huey D J and Athanasiou K A 2011 *PLoS One* **6** e27857
[41] Ballyns J J and Bonassar L J 2011 *J. Biomech.* **44** 509–16
[42] Chen P, Mei S, Xia C, Zhu R, Pang Y, Wang J, Zhang J, Shao F and Fan S 2017 *Oncotarget* **8** 30235–51
[43] Krouwels A, Melchels F P W, van Rijen M H P, Ten Brink C B M, Dhert W J A, Cumhur Öner F, Tryfonidou M A and Creemers L B 2018 *Acta Biomater.* **66** 238–47
[44] O'Conor C J, Case N and Guilak F 2013 *Stem Cell Res. Ther.* **4** 61
[45] Tuli R, Tuli S, Nandi S, Huang X, Manner P A, Hozack W J, Danielson K G, Hall D J and Tuan R S 2003 *J. Biol. Chem.* **278** 41227–36
[46] Kisiday J D, Frisbie D D, McIlwraith C W and Grodzinsky A 2009 *Tissue Eng.* A **15** 2817–24
[47] Puetzer J L and Bonassar L J 2016 *Tissue Eng.* A **22** 907–16
[48] Petri M *et al* 2012 *Knee Surg. Sports Traumatol. Arthrosc.* **20** 223–31
[49] Zielinska B, Killian M, Kadmiel M, Nelsen M and Haut Donahue T L 2009 *Osteoarthr. Cartil.* **17** 754–60
[50] Visser J, Melchels F P, Jeon J E, van Bussel E M, Kimpton L S, Byrne H M, Dhert W J, Dalton P D, Hutmacher D W and Malda J 2015 *Nat. Commun.* **6** 6933
[51] Thorpe S D, Buckley C T, Vinardell T, O'Brien F J, Campbell V A and Kelly D J 2008 *Biochem. Biophys. Res. Commun.* **377** 458–62